Journal of Saudi Chemical Society (2019) **23**, 205–214

King Saud University

Journal of Saudi Chemical Society

www.ksu.edu.sa
www.sciencedirect.com

ORIGINAL ARTICLE

Synthesis, structural characterization and biological activities of metal(II) complexes with Schiff bases derived from 5-bromosalicylaldehyde: Ru(II) complexes transfer hydrogenation

Kenan Buldurun [a], **Nevin Turan** [b,*], **Ahmet Savcı** [c], **Naki Çolak** [d]

[a] *Catalysis Research and Application Center, İnönü University, 44280 Malatya, Turkey*
[b] *Department of Chemistry, Faculty of Arts and Sciences, Muş Alparslan University, 49250 Muş, Turkey*
[c] *Department of Molecular Biology and Genetics, Faculty of Arts and Sciences, Muş Alparslan University, 49250 Muş, Turkey*
[d] *Department of Chemistry, Faculty of Arts and Sciences, Hitit University, 19100 Çorum, Turkey*

Received 18 April 2018; revised 4 June 2018; accepted 5 June 2018
Available online 28 June 2018

KEYWORDS

Antioxidant activity;
Antiradical activity;
Transition metals;
Carboxylate ligand;
Transfer hydrogenation

Abstract In this study, two novel Schiff base ligands (L^1 and L^2) derived from condensation of methyl 2-amino-6-methyl-4,5,6,7-tetrahydrothieno[2,3-c]pyridine-3-carboxylate and methyl 2-amino-6-phenyl-4,5,6,7-tetrahydrobenzo[b]thiophene-3-carboxylate, both starting matter with 5-bromo-salicylaldehyde, and their Zn(II) and Ni(II) metal complexes have been prepared using a molar ratio of ligand:metal as 1:1 except the Ru(II) complexes 1:0.5. The structures of the obtained ligands and their metal complexes were characterized by elemental analysis, FT-IR, ^{1}H NMR, ^{13}C NMR, UV–vis, thermal analysis methods, mass spectrometry, and magnetic susceptibility measurements. Antioxidant and antiradical activity of Schiff base ligands and their metal complexes were been evaluated in vitro tests. Antioxidant activities of metal complexes generally were more effectives than free Schiff bases. **1c** and **2c** were used as catalysts for the transfer hydrogenation (TH) of ketones. **1c**, **2c** complexes were found to be efficient catalyst for transfer hydrogenation reactions.

1. Introduction

Schiff bases are very significant due to their stability, chelating properties and biological applications [1]. A great deal of attention in this area has been focused on the complexes formed by transition metal ions with Schiff bases because of the presence of both nitrogen and oxygen donor atoms in the backbones of these ligands [2–4]. Schiff bases containing halogen groups and their metal complexes have a special

* Corresponding author.
E-mail address: nevintrn@hotmail.com (N. Turan).
Peer review under responsibility of King Saud University.

Production and hosting by Elsevier

https://doi.org/10.1016/j.jscs.2018.06.002

interest due to their antimicrobial properties [5]. It is also reported that salicylaldehyde derivatives, with one or more halo-atoms in the aromatic ring, shows biological activities like antitumor, antibacterial and antifungal activities [6–10]. In recent years, metal-based drugs have gained much importance in medicinal field. They are in use as medicines for the treatment of diabetes, cancer, anti-inflammatory and cardiovascular disease [11–13]. Some of Schiff bases and their transition metal complexes have also been used as drugs as bactericidal, fungicidal, anti-tubercular and antiviral agents [14–16]. Steric and electronic effects of substituent's in the coordination zone increases the activity of the metal and the other groups on ligands that not attended to coordination also may have an impact on this activity [17].

The large impact of the use of Schiff base ligands in metal complexes is evident from their advantage in various catalytic reactions such as, hydrogenation of olefins and carbonyl groups, transfer of an amino group, photochromic properties, complexing ability toward some toxic metals, etc. [18–22]. The most active and selective hydrogen transfer catalysts are ruthenium, rhodium and iridium complexes. Ruthenium complexes are preferable over those of rhodium and iridium because of their high activity and lower cost. Among the different ruthenium compounds, arene ruthenium compounds belong to a well-established family of robust metal–organic molecules that have played an important role in the development of organometallic chemistry [23].

In this study, we reported the synthesis, spectroscopic characterization, antioxidants, antiradical properties and catalytic activity of the Schiff base ligands and their Zn(II), Ni(II) and Ru(II) complexes. The ligands were two Schiff bases [(*E*)-methyl 2-(5-bromo-2-hydroxybenzylideneamino)-6-methyl-4,5,6,7-tetrahydrothieno[2,3-*c*]pyridine-3-carboxylate (L^1) and (*E*)-methyl 2-(5-bromo-2-hydroxybenzylideneamino)-6-phenyl-4,5,6,7-tetrahydrobenzo[*b*]thiophene-3-carboxylate (L^2)]. In addition, six complexes were synthesized from the reactions of L^1 and L^2 with a mixture of $ZnCI_2{\cdot}2H_2O$, $NiCI_2{\cdot}6H_2O$, and $[RuCl_2(p\text{-cymene})]_2$ metal salts. The structure of synthesized ligands and their complexes were characterized using various spectral methods. Antioxidants and antiradical activities of ligands and their complexes were discussed. The new ruthenium complexes (**1c**, **2c**) showed to be efficient catalysts for the TH of the different aromatic ketones to their corresponding secondary alcohols.

2. Experimental

2.1. Materials and physical measurements

All the chemicals and solvents used in this research were of analytical grade and used as received. Elemental analyses (carbon, hydrogen, nitrogen and sulfur) were performed on a LECO 932 CHNS analyzer. The Fourier transform infrared spectra were recorded on a Perkin Elmer FT/IR-65 spectrophotometer in the range 400–4000 cm^{-1} with a KBr disk and electronic spectra were recorded using a Shimadzu UV/Vis 1800 spectrophotometer in the range 190–1100 nm in ethanol at 300 K in 1 cm quartz cuvettes. ^1H and ^{13}C NMR spectra were recorded with a Varian AS 400 Merkur spectrometer operating at 400 MHz in $CDCl_3$ with tetramethylsilane as an internal reference. The ESI-MS spectra were recorded using LC-MS IT-TOF (HRMS) (Anadolu University). Room temperature magnetic susceptibility measurements were carried out on powdered samples using a Sherwood Scientific MX1 Model Gouy Magnetic Susceptibility Balance. The molar magnetic susceptibility (χ_M) was calculated using the equation: $\chi_M = \chi_g \times M_T$, where M_T was the formula mass of the complex. Thermogravimetric analysis (TGA) and differential thermal analysis (DTA) were carried out in nitrogen atmosphere with a heating rate of 10 °C/min. using Shimadzu DTG-60 AH (Shimadzu DSC 60 A) thermal analyzers. All catalytic reactions were monitored on an Agilent 6890 N GC system by GC-FID with a HP-5 column of 30 m length, 0.32 mm diameter and 0.25 μm film thickness. Column chromatography was performed using silica gel 60 (70–230 mesh). Solvent ratios are given as v/v.

2.2. Synthesis of Schiff base ligands (L^1 and L^2)

The Schiff base ligands have been synthesized by refluxing reaction mixture of hot ethanol solution (30 mL) of methyl 2-amino-6-methyl-4,5,6,7-tetrahydrothieno[2,3-c]pyridine-3-carboxylate (0.67 g, 0.30 mmol) with hot ethanol solution (30 mL) of 5-bromo-2-hydroxybenzaldehyde (0.60 g, 0.30 mmol) for 24 h with addition of ~ 4, 5 drops of glacial acetic acid then the color of the solution changed to orange red. Precipitate was filtered, washed with ether, and recrystallized from hot ethanol. Similarly synthesis was performed for the (L^2) using methyl 2-amino-6-phenyl-4,5,6,7-tetrahydrobenzo[b]thiophene-3-carboxylate (0.86 g, 0.30 mmol). Yield: 90%, m.p. 149–151 °C and Yield: 85%, m.p. 179–181 °C of Schiff bases (L^1 and L^2), respectively.

2.2.1. (E)-Methyl 2-(5-bromo-2-hydroxybenzylideneamino)-6-methyl-4,5,6,7-tetrahydrothieno[2,3-c]pyridine-3-carboxylate (L^1)

Anal. Calcd. for ($C_{17}H_{17}BrN_2O_3S$) (FW: 409.30 g/mol) (%): C; 49.84, H; 4.15, N; 6.84, S; 7.81. Found: C; 50.00, H; 4.18, N; 7.00, S; 7.85. FT-IR (KBr, *v* max (cm^{-1})): 3370 (OH), 3000–3030 (Ar–CH), 2937 (Alif.–CH), 1700 (C=O), 1655 (CH=N), 1598–1556 (Ar–C=C), 1321 (C-N), 1205 (C-O), 726 (C–S–C). ^1H NMR (400 Mz, $CDCl_3$): δ (ppm):12.78 (s, 1H, Ar. C-OH), 8.34 (s, H, N=CH), 7.39–6.83 (m, 3H, Ar-H), 3.49–2.66 (m, 6H, CH_2), 2.41 (s, 3H, N-CH_3), 1.32 (s, 3H, –OC=O-CH_3). ^{13}C NMR (400 Mz, $CDCl_3$): δ (ppm): 162.98 (C=O), 160.02 (CH=N), 157.46 (C-OH), 133.96–152.92 ($C_{2\text{-thiophene}}$), 110.58–129.41 ($C_{1\text{-benzene}}$), 14.36, 26.87, 60.97 ($C_{piperidine}$), 52.16 (OCH_3), 45.49 (N-CH_3). UV–vis bands (λ_{max}, nm, (ε, M^{-1} cm^{-1}): Benzene, imin $\pi \rightarrow \pi^*$, 270 (79.200), 291 (109.95); $n \rightarrow \pi^*$, 323 (70.05), 402 (187.75). Mass Spectrum [ESI]: *m/z* 410.10 (Found) $[L + H]^+$.

2.2.2. (E)-methyl 2-(5-bromo-2-hydroxybenzylideneamino)-6-phenyl-4,5,6,7-tetrahydrobenzo[b]thiophene-3-carboxylate (L^2)

Anal. Calcd. for ($C_{23}H_{20}BrNO_3S$) (FW: 470.33 g/mol) (%): C; 58.73, H; 4.29, N; 2.98, S; 6.82. Found: C; 58.78, H; 4.25, N; 2.75, S; 6.93. FT-IR (KBr, *v* max (cm^{-1})): 3381 (OH), 3100, 3020 (Ar–CH), 2945, 2876 (Alif.–CH), 1706 (C=O), 1601 (CH=N), 1552 (Ar–C=C), 1198 (C-O), 722 (C–S–C). ^1H NMR (400 Mz, $CDCl_3$): δ (ppm) = 12.78 (s, 1H, Ar.–COH), 8.32 (s, H, N=CH), 7.36–7.16 (m, 8H, Ar-H), 3.02–2.70

(m, 6H, CH_2), 1.88 (m, 1H, C-CH-C), 1.35 (s, 3H, –OC═O-CH_3). ^{13}C NMR (400 Mz, $CDCl_3$): δ (ppm) = 163.27 (C═O), 159.97 (CH═N), 157.26 (C-OH), 135.90–152.40 ($2C_{thiophene}$), 110.58–135.95 ($C_{benzene}$), 26.66, 61.01 ($C_{siklohexane}$), 14.10 (O-CH_3). UV–vis bands (λ_{max}, nm, (ε, M^{-1} cm^{-1}): Benzene, imin $\pi \rightarrow \pi^*$, 272 (21350), 289 (26700); $n \rightarrow \pi^*$, 331 (15300), 402 (31450). Mass Spectrum [ESI]: *m/z* 470.38 (Calcd.), 471.10 (Found) $[L + H]^+$.

2.3. Preparation of the complexes

The metal complexes were prepared by adding stoichiometric quantities to a hot ethanol solution (30 mL) containing 20 mmol of ligand and ethanol solution (20 mL) of metal chlorides ($NiCl_2 \cdot H_2O$ and $ZnCl_2 \cdot 2H_2O$) for 20 mmol. For ruthenium complex 10 mmol $[RuCl_2(p\text{-cymene})]_2$ was used. The reaction mixture was stirred for 24 h. The residue was washed with diethyl ether (20 mL) and dried under vacuum. The desired products were recrystallized in ethanol and dried at room temperature. m.p. > 200 °C (Yield: 70–80%). On the basis of their physiochemical studies, the suggested structure of the complexes is given Fig. 1.

$[NiL^1(H_2O)_3]\cdot 3H_2O\cdot Cl$: FW: 610.49 g/mol. FT-IR (KBr, *v*max (cm^{-1})): 3400 $(OH)_{broad}$, 3100 $(Ar–CH)_{broad}$, 2967 (CH), 1704 (C═O), 1650 (CH═N), 1593–1562 (Ar–C═C), 1308 (C-N), 1213 (C-O), 722 (C–S–C), 563, 520 (M−O), 490, 463 (M−N). Anal. Calcd. for ($C_{17}H_{28}N_2SO_9BrClNi$): C; 33.44, H; 4.59, N; 4.59, S; 5.24. Found: C; 33.74, H; 4.26, N; 4.62, S; 5.27. UV–vis bands (λ_{max}, nm, (ε, M^{-1} cm^{-1}): Azomethine; $n \rightarrow \pi^*$, 270 (23.75), 296 (14.30), 362 (12.35), 504 (24.60), 753 (37.65), 854 (42.70), 954 (47.70), 1039 (51.95) L → M, LLCT. Mass Spectrum [ESI]: *m/z* 521.99 (calcd.), 521.98 (found) $[M-3H_2O-Cl + H]^{+2}$. Color: Dark Brown.

$[ZnL^1(H_2O)_2Cl]\cdot 4H_2O$: FW: 617.19 g/mol. FT-IR (KBr, *v*max (cm^{-1})): 3411 $(OH)_{broad}$, 3040 $(Ar–CH)_{broad}$, 2979 (Alif.–CH), 2743 (Aldehyde–CH), 1698 (C═O), 1638 (CH═N), 1598–1577 (Ar–C═C), 1382 (C-N), 1210 (C-O), 722 (C–S–C), 544, 529 (M−O), 489 (M−N); Anal. Calcd. for ($C_{17}H_{28}N_2SO_9BrClZn$): C; 33.11; H; 4.54, N; 4.54, S; 5.19. Found: C; 33.00, H; 4.55, N; 4.86, S; 5.30. UV–vis bands (λ_{max}, nm, (ε, M^{-1} cm^{-1}): Benzene, imin; 287 (44.70) $\pi \rightarrow \pi^*$, 339 (32.55), 402 (49.90), 963 (2 0 0) L → M, LLCT. Mass Spectrum [ESI]: *m/z* 509.69 (calcd.), 509.05 (found) $[M-4H_2O-Cl]^+$. Color: Brick color.

$[RuL^1Cl]\cdot 5H_2O$: FW: 768.87 g/mol. FT-IR (KBr, *v*max (cm^{-1})): 3407 $(OH)_{broad}$, 3100 (Ar–CH), 2960 (Alif.–CH), 1699 (C═O), 1670 (CH═N), 1594–1570 (Ar–C═C), 1316 (C-N), 1200 (C-O), 726 (C–S–C), 546 (M−O), 480, 455 (M−N), 465 (Ru–Cl). Anal. Calcd. for ($C_{27}H_{40}N_2SO_8$-BrClRu): C; 42.13, H; 5.53, N; 3.64, S; 4.16. Found: C; 42.37, H; 5.60, N; 3.66, S; 4.10. UV–vis bands (λ_{max}, nm, (ε, M^{-1} cm^{-1}): İmin; 337 (18.25) $\pi \rightarrow \pi^*$, 405 (21.100), 547 (5.200) L → M. Mass Spectrum [ESI]: *m/z* 545.87 (calcd.), 545.67 (found) $[M + H\text{-}5H_2O\text{-p-cymene}]^+$. Color: Black.

$[NiL^2(H_2O)_3]\cdot 3H_2O\cdot Cl$: FW: 671.57 g/mol. FT-IR (KBr, *v*max (cm^{-1})): . FT-IR (KBr, *v*max (cm^{-1})): 3491$(OH)_{broad}$, 3040 $(Ar–CH)_{broad}$, 2936 (Alif.–CH), 2770 (Aldehyde–CH), 1704 (C═O), 1596 (CH═N), 1552 (Ar–C═C), 1386 (C-N), 1167 (C-O), 700 (C–S–C), 540 (M−O), 468 (M−N); Anal. Calcd. for ($C_{23}H_{31}BrClNO_9SNi$): C; 41.13; H; 4.61, N; 2.08, S; 4.76. Found: C; 41.16, H; 4.41, N; 2.11, S; 4.77. UV–vis bands (λ_{max}, nm, (ε, M^{-1} cm^{-1}): Benzene, imin; 271 (33.70), 297 (24.55) $\pi \rightarrow \pi^*$, 366 (15.05), 500 (3500), 786 (39.30), 885 (42.75), 954 (47.70), 1038 (51.90) L → M, LLCT. Mass Spectrum [ESI]: *m/z* 583.07 (calcd.), 583.00 (found) $[M + H\text{-}3H_2O\text{-}Cl]^{+2}$. Color: Dark Brown.

$[ZnL^2(H_2O)_2Cl]\cdot 3H_2O$: FW: 660.31 g/mol. FT-IR (KBr, *v*max (cm^{-1})): 3410 $(OH)_{broad}$, 3040 $(Ar–CH)_{broad}$, 2936 (Alif.–CH), 2740 (Aldehyde–CH), 1700 (C═O), 1598 (CH═N), 1550 (Ar–C═C), 1372 (C-N), 1196 (C-O), 700 (C–S–C), 539 (M−O), 495–473 (M−N); Anal. Calcd. for ($C_{23}H_{29}$-$BrClNO_8SZn$): C; 41.84, H; 4.43, N; 2.12, S; 4.86. Found: C; 41.76, H; 4.51, N; 2.06, S; 4.47. UV–vis bands (λ_{max}, nm, (ε, M^{-1} cm^{-1}): Benzene, imin; 291 (67.50) $\pi \rightarrow \pi^*$, 387 (47.00), 480 (6000) L → M. Mass Spectrum [ESI]: *m/z* 661.27 (calcd.), 661.18 (found) $[M + H]^+$. Color: Orange.

$[RuL^2Cl]\cdot 2H_2O$: FW: 775.78 g/mol. FT-IR (KBr, *v*max (cm^{-1})): 3411 $(OH)_{broad}$, 3170 (Ar–CH), 2960 (Alif.–CH), 1706 (C═O), 1599 (CH═N), 1552 (Ar–C═C), 1323 (C-N), 1201 (C-O), 722 (C–S–C), 538 (M−O), 470 (Ru–Cl), 457 (M−N). Anal. Calcd. for ($C_{33}H_{37}BrClNO_5RuS$): C; 51.04, H; 4.76, N; 1.80, S; 4.12. Found: C; 51.39, H; 4.79, N; 1.78, S; 4.14. UV–vis bands (λ_{max}, nm, (ε, M^{-1} cm^{-1}): İmin; 342 (3790) $\pi \rightarrow \pi^*$, 753 (1 0 0), 855 (1 5 0), 954 (8 5 0) L → M, LLCT. Mass Spectrum [ESI]: *m/z* 570.85 (calcd.), 573.19 (found) $[M-2H_2O-Cl-p-cymene]^+$. Color: Black.

2.4. Antioxidant activity assays

2.4.1. Total antioxidant activity determination by ferric thiocyanate method

Ferric thiocyanate method [24] modified by Gülçin [25] used for determine the antioxidant activity of ligands, their Ni(II), Zn(II) and Ru(II) complexes. We used BHA butylated hydroxyanisole (BHA) and butylated hydroxytoluene (BHT) as standards. The most commonly used antioxidants at the present time are butylated hydroxyanisole (BHA), butylated hydroxytoluene (BHT), propyl gallate and *tert*-butylhydroquinone [26]. 10 mg of ligand and complexes were dissolved in 10 mL ethanol as stock. Then, the solution which contains the same concentration of stock L^1, L^2 and their metal complexes solution or standard samples (100 mg/mL) in sodium phosphate buffer (0.04 M, pH 7.0, 2.5 mL) was added to linoleic acid emulsion in sodium phosphate buffer (0.04 M, pH 7.0, 2.5 mL). 5 mL of the linoleic acid emulsion was prepared by mixing and homogenizing 15.5 mL of linoleic acid, 17.5 mg of Tween-20 as emulsifier, and 5 mL phosphate buffer (pH 7.0). Then, 5 mL control was composed of 2.5 mL of linoleic acid emulsion and 2.5 mL, 0.04 M sodium phosphate buffer (pH 7.0). The mixed solution (5 mL) was incubated in a polyethylene flask at 37 °C. The peroxide level was determined by reading the absorbance at 500 nm after reaction with $FeCl_2$ and thiocyanate at intervals during the incubation. During the linoleic acid oxidation, peroxides are formed and that leads to oxidation of Fe^{2+} to Fe^{3+}. The latter ions form a complex with ammonium thiocyanate and this complex had a maximum absorbance at 500 nm. This stage was repeated every 10 h until the control reached its maximum absorbance value. The percentage inhibition values were calculated at this point (30 h). High absorbance indicates high linoleic acid emulsion peroxidation. The percentage inhibition of lipid peroxidation in the linoleic acid emulsion was calculated by the following equation:

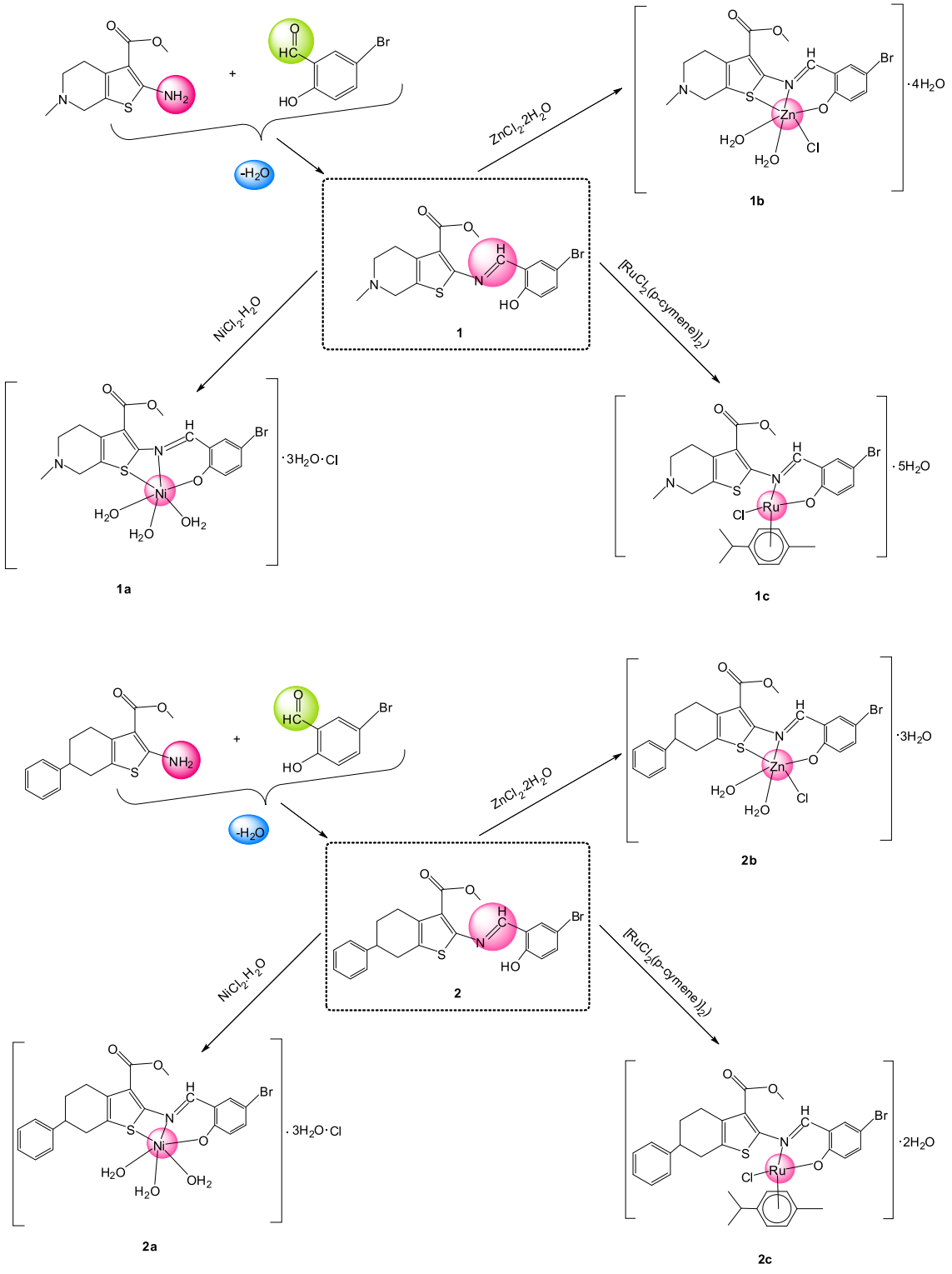

Fig. 1 The general scheme of ligands and their metal complexes.

Inhibition of lipid peroxidation (%) = 100 − (As/Ac × 100)

Ac: Absorbance of the control; As: Absorbance of samples

2.4.2. Total reduction capability

The reducing power of ligands, complexes and standard samples (BHA and BHT) were determined by the method of Oyaizu [27] with slight modification [28]. This assay is based on the principle that substances that have high reduction potential react with potassium ferricyanide (Fe^{3+}) and forms potassium ferrocyanide (Fe^{2+}) which then reacts with ferric chloride. Different concentrations of L^1, L^2, their complexes and standard samples (25–100 mg/mL) in 1 mL of distilled water were mixed with phosphate buffer (2.5 mL, 0.2 M,

pH 6.6) and potassium ferricyanide [$K_3Fe(CN)_6$] (2.5 mL, 1%). The mixture was incubated at 50 °C for 20 min. Aliquots (2.5 mL) of trichloroacetic acid (10%) were added to the mixture. The supernatant (2.5 mL) was mixed with distilled water (2.5 mL) and $FeCl_3$ (0.5 mL, 0.1%), and the absorbance was measured at 700 nm in a spectrophotometer. Increased absorbance of the reaction mixture indicates an increase in reduction capability.

2.5. Antiradical activity

2.5.1. 1,1-Diphenyl-2-picryl-hydrazil (DPPH) free radical scavenging activity

The free radical scavenging activity of compounds was determined by the 1,1-diphenyl-2-picryl-hydrazil (DPPH) that described by Blois [29]. In its radical form DPPH· absorbs at 517 nm, but upon reduction by an antioxidant or a radical species its absorption decreases. Briefly, 0.1 mM solution of DPPH in ethanol was prepared and 1 mL of this solution was added 3 mL of ligands, complexes and standards at different concentrations (25–100 μg/mL). Thirty minutes later, the absorbance was measured at 517 nm. Lower absorbance of the reaction mixture indicates higher free radical scavenging activity.

2.6. General procedure for the transfer hydrogenation of ketones

The catalytic hydrogen transfer reactions were carried out in a closed Schlenk flask under argon atmosphere. A mixture of the required ketone (1 mmol), catalyst Ru(II) complexes **1c**, **2c** (0.01 mmol) and KOH (4 mmol) were heated to reflux in 5 mL of *i*-PrOH for 8 h. Then the solvent was removed under vacuum, and the residue was extracted with ethyl acetate/hexane (1:5), filtered through a pad of silica gel with copious washings, concentrated and purified by flash chromatography on silica gel. The product distribution was determined by ^{1}H NMR spectroscopy, GC and GC–MS.

3. Results and discussion

3.1. Infrared spectra

The typical infrared spectrum of the Schiff base ligands have been represented in experimental section. The most important IR bands of Schiff bases showed a broad band at 3381–3370 cm^{-1}, strong bands at 1700–1706, 1655–1601, 1205–1198 and 726–722 cm^{-1} range assigned to ν(OH), ν(C═O), ν(CH═N), ν(C—O) and ν(C—S—C) vibrations, respectively. The bands at 1706, 1700 cm^{-1} in the ligands were still in the same position in the complexes indicating the non-involvement of the carbonyl ν(C═O) in coordination. The IR broad bands of metal complexes in the range of 3491–3222 cm^{-1} indicate the presence of coordinated/lattice water molecules as also supported by thermal analysis [18,19]. The bands appearing in the spectra of the ligands at 3381, 3370 cm^{-1} were assigned to ν(OH) vibrations and this bands were absent in the spectra of all the complexes. The disappearance of the band for the □(OH) vibration in the spectra of the complexes indicated the deprotonation of the phenolic proton, followed by coordination of the phenolic oxygen with the metal atoms [30]. The C—O (phenolic) modes of the ligands appear at 1205–1198 cm^{-1} range, shifted frequency in the complexes indicate the complexes formation via deprotonation of phenolic OH [19,31]. The ν(CH═N) observed at 1655–1601 cm^{-1} range in the spectra of the ligands showed a shift by 2–17 cm^{-1} in all the complexes. These were show the participation of the azomethine nitrogen in coordination [9]. The nonligand bands 520 to 563 cm^{-1} and 455 to 495 cm^{-1} were assigned to M − O and M − N, respectively [32,33]. The observed band in 470, 465 cm^{-1} in the Ru(II) complexes were assigned to the ν (Ru–Cl) vibrations [34]. The ν(C—S—C) stretching band in the ligands was observed at 726, 722 cm^{-1} [13–15]. This band was shifted to higher or lower frequency values upon complexation suggesting coordination via the C—S—C group, except for that of Ru(II) complexes.

3.2. Magnetic susceptibility and electronic spectra measurements

Electronic absorption spectra for L^1, L^2 and their complexes were recorded in $1x10^{-5}$ M EtOH solutions. The electronic spectral data of the ligands showed four bands in the UV region. The bands around 270–291 nm can be assigned to intra ligand of $\pi \rightarrow \pi^*$ transition. The other bands observed in the region of 323, 331 and 402 nm were attributed to $n \rightarrow \pi^*$ electronic transitions. Ni(II), Zn(II) and Ru(II) complexes showed bands at 291–270, 387–297 and 402 nm which were attributed to the $\pi \rightarrow \pi^*$and $n \rightarrow \pi^*$ transitions, within the ligand. The spectra of the complexes further display bands in the range 405–480 and 500–547 nm, which might be assigned to ligands to metal ions (L → M) and ligand-to-ligand (LLCT) charge transfer transitions [35–37].

Ni(II) complexes with octahedral geometries showed differences in their UV–vis spectra. For octahedral complexes, the *d-d* bands were weak and the spectra usually show three absorptions at around 1039–753, 954–504 and 504–362 nm. These bands were assigned to $^3A_{2g}(F) \rightarrow {}^3T_{1g}(F)$, $^3A_{2g}(F) \rightarrow {}^3T_{2g}(F)$ and $^3A_{2g}(F) \rightarrow {}^3T_{1g}(P)$ transitions, respectively [38]. The measured magnetic moment value were of Ni(II) complexes 3.10 and 2.80B.M., respectively [39]. Zn(II) complexes were diamagnetic and show absorptions in the region 287–480 nm due to intra ligand/charge transfer transitions, suggesting the presence of d^{10} octahedral Zn(II) [40,41]. Ru(II) complexes were diamagnetic, indicating the presence of ruthenium in +2 oxidation state in all the complexes. Their geometries were octahedral [42].

3.3. ^{1}H and ^{13}C NMR spectra

The ^{1}H NMR spectrum of Schiff base ligands was recorded in chloroform ($CDCl_3$) solution using tetramethylsilane (TMS) as internal standard. In the ^{1}H NMR spectrum of L^1, ligand the following signals was observed: singlet signal at δ = 12.78 ppm was attributed to hydrogen of Ar-OH group (s, H). The signal of N═CH was observed at 8.34 (s, H) ppm. The signals of aryl-H were seen at δ = 7.39–6.83 ppm (m, 3H). The signal of $3CH_2$ was observed at 3.49–2.66 ppm (m, 6H). The signal of N-CH_3 was observed at 4.41 ppm (s, 3H). The signal of carbonyl-OCH_3 was observed at 1.32 ppm (s, 3H). The ^{1}H NMR spectra of the L^2 are listed in experimental section. The spectra of the Zn(II) complexes were examined in comparison with those of the ligands. Upon examinations it was found

that the phenolic-OH signal, appeared in the spectrum of L^1 and L^2 ligands at 12.78 ppm is completely disappeared in the spectra of its Zn(II) complexes indicating that the OH proton is removed by the complexation with Zn(II) ions. Also the signal observed at 3.80–4.24 ppm with an integration corresponding to twelve protons in case of Zn(II) complexes, is assigned to six water molecules.

The ^{13}C NMR spectra of the Schiff base ligands have similar properties. The measured chemical shifts of all carbon atoms for ligands were listed in experimental section. In ^{13}C NMR, the signal due to the azomethine carbon atom was observed at 160.02, 159.97 ppm, respectively. In the Zn(II) complexes' spectrum, the two azomethine carbon signals appear at 158.40, 157.32 ppm, respectively. This signals are shifted upfield in Zn(II) complexes' spectrum which indicates the participation of azomethine groups in complex formation [43]. The shift of the peaks indicated that the complexation reactions were successful for L^1 and similarly for L^2.

3.4. Thermal analysis

The thermal degradation of Ni(II), Zn(II) and Ru(II) complexes was studied using thermogravimetric techniques and a temperature range of 25–800 °C. The lattice water molecules are lost at low temperature (30–150 °C), whereas the coordinated water molecules are lost at high temperatures (160–300 °C).

The TGA curves of the metal complexes give two or three stage decomposition pattern within the ranges 25–800 °C. The first degradation stage takes place in the range of 40–390 °C which is a weight loss 23.49% and associated with exothermic peaks at 150 and 240 °C with endothermic peak at 260 and 300 °C. The second degradation stage takes place in the range of 393–800 °C which is a weight loss 64.26% and associated with exothermic peaks at 646 and 735 °C with endothermic peak at 500 °C for Ni(II) metal complexes. For Zn(II) metal complex, the first degradation stage takes place in the range of 70–390 °C which is a weight loss 23.23% and associated with endothermic peak at 256 and 355 °C, the second degradation stage takes place in the range of 400–800 °C which is a weight loss 63.58% and associated with exothermic peaks at 651 and 700 °C with endothermic peak at 490 and 710 °C. For ruthenium metal complex, the first degradation stage takes place in the range of 30–316 °C which is a weight loss 11.70%, the second degradation stage takes place in the range of 320–390 °C which is a weight loss 22.03% and associated with exothermic peaks at 438 °C with endothermic peak at 570 °C, the third degradation stage takes place in the range of 560–800 °C which is a weight loss 51.03% and associated with exothermic peaks at 630 °C with endothermic peak at 684 and 700 °C. The TGA curves of Ni(II), Zn(II) and Ru (II) complexes indicate a total weight loss of 87.75, 86.81, 84.76% up to 800 °C, respectively. Maximum and gradual weight loss in the range of 360–800 °C is attributable to the decomposition of ligand moiety. The residues at 750–800 °C indicate the nonvolatile metal component present in the complex [44].

Decompositions were observed at about the same rates for L^2 as well. The lattice water molecules were removed in the first stage, coordinated water molecules and Cl groups were removed in the second stage and the rest of the ligand was removed in the third stage. The last decomposition products are metal oxides.

3.5. Mass spectral analysis

ESI–Mass spectral analysis of the complexes was studied in order to confirm the molecular masses of the complexes. The molecular ion peaks, $[M^+]$ appeared at m/z = 509.05–661.18 confirm the stoichiometry of the complexes, respectively.

3.6. Total reductive capability using the potassium ferricyanide reduction method

Antioxidant activities of L^1 and L^2 ligands and their Ni(II), Zn (II) and Ru(II) complexes and standards (BHA, BHT) shown according to the FRAP (Ferric Reducing Antioxidant Power) method in Fig. 2.

Reduction potential of the samples in different concentrations (25 μL, 50 μL ve 100 μL) was determined by measuring absorbance at 700 nm. Power reduction activity of samples with standard antioxidants in 100 μL was determined respectively as BHA > BHT > L^1-Ni ≥ L^1-Zn > L^1 ≥ L^1-Ru. The

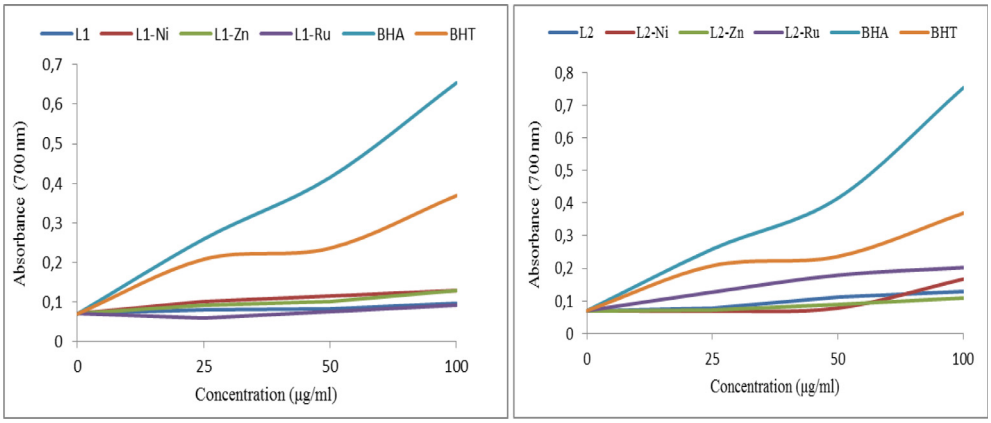

Fig. 2 Total reductive potential of different concentrations (25–100 mg/mL) of ligands and their complexes, BHA and BHT using the Fe^{3+}-Fe^{2+} transformation.

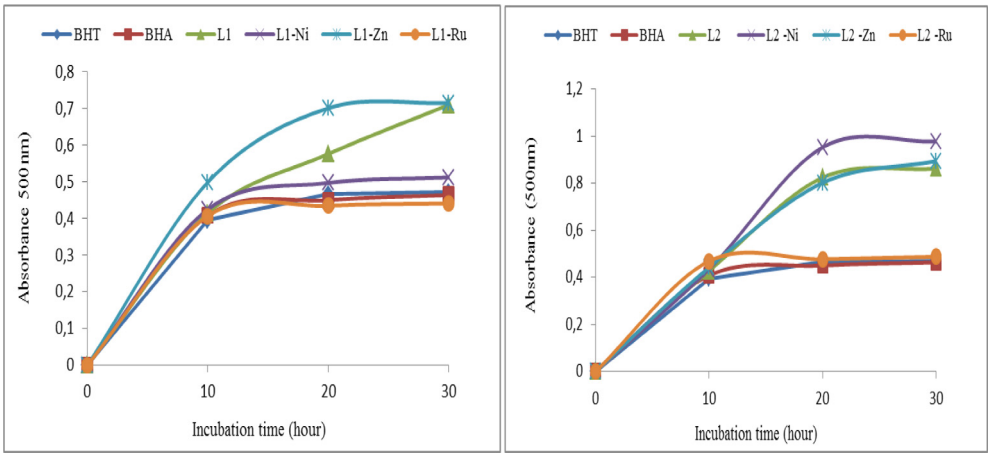

Fig. 3 Total antioxidant activities of ligands and their complexes, BHA and BHT at the same concentration (100 mg/mL) in the linoleic acid emulsion system by the ferric thiocyanate method.

results of other ligand and its complexes observed were highest in BHA > BHT > L^2-Ru > L^2-Ni > $L^2 \geq L^2$-Zn.

3.7. Total antioxidant activity determination in a linoleic acid emulsion by the ferric thiocyanate method

Lipid peroxidation involves a series of free radical mediated chain reactions and is also associated with several types of biological damage. The role of free radicals and ROS is becoming increasingly recognized in the pathogenesis of many human diseases, including cancer, aging, and atherosclerosis [37]. Total antioxidant activity of samples and standards was determined by the ferric thiocyanate method in the linoleic acid system. The effects of the same concentration (100 mg/mL) of samples and standards on lipid peroxidation of linoleic acid emulsion shown in Fig. 3 were found to be L^1-Ru (63.41%) > BHA (62.15%) > BHT (60.81%) > L^2-Ru (59.88%) > L^1-Ni (58.20%) > L^1 (51.55%) > L^1-Zn (41.04%) > L^2-Zn (32.55%) > L^2 (30.69%) > L^2-Ni (19.85%).

3.8. DPPH free radical scavenging activity

DPPH is usually used as a reagent to evaluate free radical scavenging activity of antioxidants.

In the Fig. 4, the DPPH free radical scavenging activity of L^1 and L^2 ligands, their complexes and standard antioxidants (BHA and BHT) are shown like that: BHA (62.92%) > L^2-Ru (60.31%) > BHT (55.31%) > L^2-Zn (26.65%) > L^1-Zn (17.27%) > L^1 (3.88%) ≥ L^2-Ni (3.85%) > L^1-Ru (3.04%) > L^2 (1.31%) > L^1-Ni(0.19%).

3.9. Catalytic transfer hydrogenation

In recent times, the TH of ketones to alcohols has been extensively investigated. At the same time, studies are continuously being aimed at obtaining better catalysts. In the present work, we synthesized of novel two ruthenium(II) arene complexes bearing pyridine-3-carboxylate and thiophene-3-carboxylate **1c**, **2c** (L^1-Ru, L^2-Ru). The complexes were used as catalysts for the TH of ketone derivatives. The reaction conditions for this important process are economic, relatively mild and environmentally friendly. The volatile acetone product can also be easily removed to shift an unfavorable equilibrium [45,46]. So the performances of the TH catalysts as starting point were scanned using acetophenone as a model substrate (Table 1). The catalytic performance of the half sandwich ruthenium complexes was evaluated in the reduction in acetophenone derivatives in the presence of different bases like KOH, NaOH,

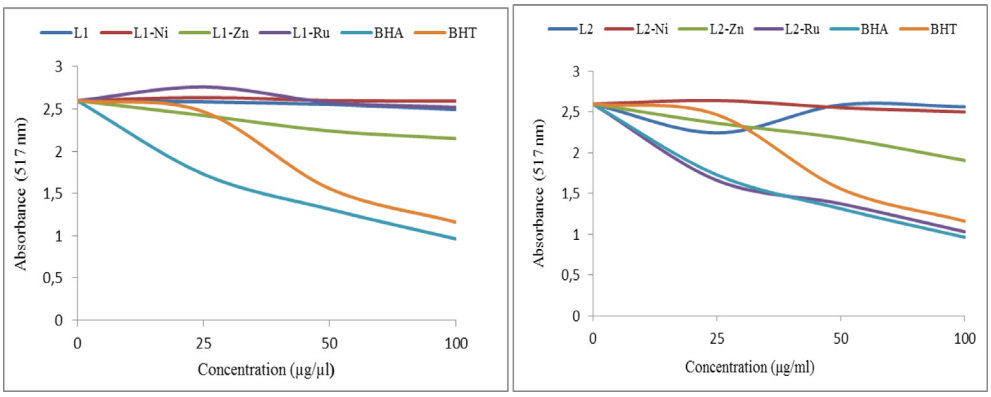

Fig. 4 DPPH·free radical scavenging activity of ligands and their complexes, BHA and BHT.

$KOBu^t$ and K_2CO_3, NaOH and KOH under homogeneous conditions. The conversion rates varied significantly with the base used and a diversity of bases KOH, NaOH, K_2CO_3, $KOBu^t$, NaOAc, Cs_2CO_3 were screened. The conversions were found to be very effective when KOH was studied as base. In addition, the choice of base, such as different bases had a remarkable influence on the conversion, [45,47]. Additionally, as can be inferred from the Table 1, the presence of base is necessary to observe appreciable conversions [48,49]. In the absence of a base no TH of the ketones was observed. Moreover, the base facilitates the formation of ruthenium alkoxide by abstracting the proton from isopropanol, different bases were used as promoters in the transfer hydrogenation of ketones. This study confirms the need of a base in enough amount for the reaction to maintained efficiently. Optimization studies show that 2-propanol is the best solvent and 4 mmol of KOH is sufficient for the present catalytic system. Various ketones have been selectively converted into corresponding alcohols (Table 2) with 1 mol% of catalyst (Table 1). As shown in Table 1, the half-sandwich ruthenium complex **1c** was found to be very active toward the reduction in acetophenone compounds. Then, we chose **1c** as the best catalyst to test the influence of solvents, reaction temperature and catalysts loading on reaction yield (Table 1). The optimized results were obtained when 4-bromoacetophenone was allowed to react with 0.01 mmol complex **1c** at 80 °C in the presence of four equivalent of KOH in i-PrOH solvent. The conversion of 4-chloroacetophenone is the fastest, giving complete conversion to the corresponding alcohol at 8 h under the selected operating conditions [50] (Table 2).

Table 1 Optimization of catalytic transfer hydrogenation.

Entry	Substrate	Product	Catalyst	Base	Yield (%)
1	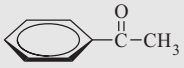	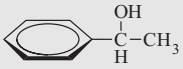	**1c**	KOH	81
2			**1c**	NaOH	55
3			**1c**	K_2CO_3	51
4			**1c**	$KOBu^t$	42
5			**1c**	NaOAc	37
6			**1c**	Cs_2CO_3	26
7			absence of **1c**	KOH	–

Reaction conditions: Ketones (1 mmol), bases (4 mmol), catalyst 1c (0.01 mmol), 2-propanole (5 mL), stirring for 8 h, 80 °C. Yield is determined by GC.

Table 2 Transfer hydrogenation of ketones catalyzed by **1c**, **2c** complex.

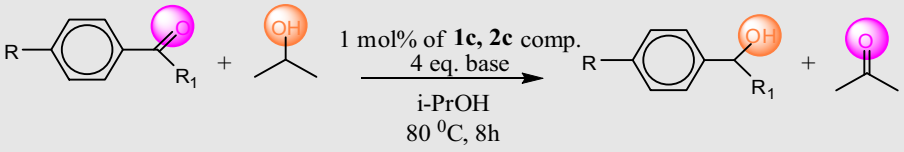

Entry	Substrate	Product	Catalyst	Base	Yield (%)
1	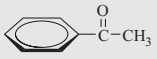	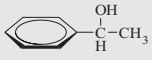	**1c**	KOH	81
2			**2c**	KOH	70
3		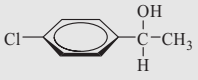	**1c**	KOH	100
4			**2c**	KOH	84
5		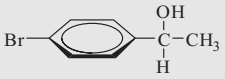	**1c**	KOH	98
6			**2c**	KOH	98
7			**1c**	KOH	41
8			**2c**	KOH	44
9	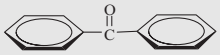	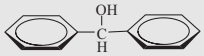	**1c**	KOH	97
10			**2c**	KOH	98
11	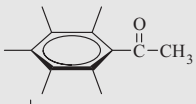	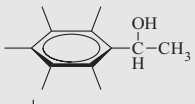	**1c**	KOH	100
12			**2c**	KOH	100
13	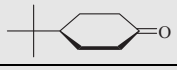		**1c**	KOH	44
14			**2c**	KOH	40

Reaction conditions: Ketones (1 mmol), bases (4 mmol), catalyst **1c**, **2c** (0.01 mmol), 2-propanole (5 mL), stirring for 8 h, 80 °C. Yield is determined by GC.

These complexes showed good catalytic activity on the reduction in ketones to their corresponding alcohols. It was observed that the conversion is dependent on the substituent present on the acetophenone ring. The conversion of ketone to secondary alcohol in the case of acetophenone was 81–70% (8h) (Table 2, entries 1,2), which takes place at a faster rate than that for 4-methoxy acetophenone (41%) (Table 2, entry 7). The presence of electron withdrawing (Cl, Br) substituent on acetophenone (Table 2, entries 3–6) has not very significant effect on the reduction in ketones to their corresponding alcohols. The maximum conversion of 4-chloroacetophenone to corresponding alcohol was achieved over a period of 8 h 100% conversion (Table 2, entry 3). 4-methoxy acetophenone was converted to its corresponding alcohol in 41% conversion (Table 2, entry 7). The p-substituted acetophenone in the presence of an electron-withdrawing substituent (bromo, chloro) on the aryl ring gave higher conversions (Table 2, entries 3–5), when compared to that of acetophenone (Table 2, entries 1, 2), while presence of an electron-donating substituent (methoxy or *tert*-butyl) on the ring decreased the conversion (Table 2, entries 7, 8, 13, 14). It was also found that the best conversion was obtained (100%) in spite of steric effect of the pentamethylbenzyl group aromatic ring (Table 2, entries 11, 12). The transfer hydrogenation wasn't observed in the absence of catalyst (Table 1 – entry 7).

The results obtained from the optimization studies indicate clearly that excellent conversion (Table 2, entries 1,3–6,9,10,11, 12) was achieved in the reduction in acetophenone its corresponding alcohol when **1c**, **2c** were used as the catalytic precursor with 0.1 mol% catalyst in 2-propanol, containing KOH as base, refluxed for 8 h at 80 °C.

4. Conclusion

Novel ligands and their complexes were prepared and characterized. The results of this investigation support the suggested structures of the metal complexes. It was obvious from this study that only mononuclear complexes were obtained. The IR spectral studies reveal that ligands coordinated to the metal ions via phenolic –OH, CH═N and the S atom of the thiophene moiety. The metal cations have octahedral geometry. According to the results of our study, we can say that metal complexes generally have better antioxidant effect than ligands. However, when we consider all the methods, we have determined that the L^2-Ru complex is more effective than other metal complexes and is close to the standards. **1c**, **2c** complexes were competent catalysts for transfer hydrogenation reactions.

Conflict of interests

We (Kenan Buldurun, Nevin Turan, Ahmet Savcı, Naki Çolak,) declare that there is no conflict of interests regarding the publication of this article.

References

[1] S. Kundu, A.K. Pramanik, A.S. Mondal, T.K. Mondal, Ni(II) and Pd(II) complexes with new N, O donor thiophene appended Schiff base ligand: synthesis, electrochemistry, X-ray structure and DFT calculation, J. Mol. Struct. 1116 (2016) 1–8.

[2] A.A. Abdel Aziz, A.N.M. Salem, M.A. Sayed, M.M. Aboaly, Synthesis, structural characterization, thermal studies, catalytic efficiency and antimicrobial activity of some M(II) complexes with ONO tridentate Schiff base N-salicylidene-o-aminophenol (saphH2), J. Mol. Struct. 1010 (2012) 130–138.

[3] Z.L. You, H.L. Zhu, W.S. Liu, Syntheses, crystal structures, and antibacterial activities of four Schiff base copper(II), zinc(II), and cadmium(II) complexes derived from 2-[(2-dimethylaminoethylimino)methyl]phenol, Z. Anorg Allg Chem. 630 (2004) 1617.

[4] A. Gölcü, M. Tümer, H. Demirelli, R.A. Wheatley, Cd(II) and Cu(II) complexes of polydentate Schiff base ligands: synthesis, characterization, properties and biological activity, Inorg. Chim. Acta 358 (2005) 1785.

[5] K.T. Samina, A.Y. Abhijit, S.B. Ratnamala, Synthesis and characterization of a novel Schiff base of 1,2-diaminopropane with substituted salicyaldehyde and its transition metal complexes: single crystal structures and biological activities, J. Mol. Struct. 1152 (2018) 223–231.

[6] R.C. Maurya, P. Patel, S. Rajput, Synthesis and characterization of n-(o-vanillinidene)-p-anisidine and N, N′-bis(o-vanillinidene)ethylenediamine and their metal complexes, Synth. React. Inorg. Met. 33 (2003) 817–836.

[7] U. Bohme, B. Gunther, Five and six-coordinate silicon complexes with an O, N, O′-chelating ligand derived from o-hydroxyacetophenone–N-(2-hydroxyethyl)imine, Inorg. Chem. Commun. 10 (2007) 482–484.

[8] L.C. Felton, J.H. Brewer, Action of substituted salicylaldehydes on bacteria and fungi, Science 105 (1947) 409–410.

[9] K.N. Kumar, R. Ramesh, Synthesis, luminescent, redox and catalytic properties of Ru(II) carbonyl complexes containing $2N_2O$ donors, Polyhedron 24 (2005) 1885–1892.

[10] A.N. Kursunlu, E. Guler, F. Sevgi, B. Ozkalp, Synthesis, spectroscopic characterization and antimicrobial studies of Co (II), Ni(II), Cu(II) and Zn(II) complexes with Schiff bases derived from 5-bromo-salicylaldehyde, J. Mol. Struct. 1048 (2013) 476–481.

[11] S.P. Fricker, Metal based drugs: from serendipity to design, Dalton Trans. 43 (2007) 4903–4917.

[12] R.R. Crichton, D.T. Dexter, R.J. Ward, Metal based neurodegenerative diseases–from molecular mechanisms to therapeutic strategies, Coord. Chem. Rev. 252 (2008) 1189–1199.

[13] R. Cini, G. Tamasi, S. Defazio, M.B. Hursthouse, Unusual coordinating behavior by three non-steroidal anti-inflammatory drugs from the oxicam family towards copper(II). Synthesis, X-ray structure for copper(II)-isoxicam, -meloxicam and -cinnoxicam-derivative complexes, and cytotoxic activity for a copper(II)-piroxicam complex, J. Inorg. Biochem. 101 (2007) 1140–1152.

[14] A. Rauf, S. Afzal, S.M. Khurram, K. Abdul Aziz, A. Rashda, A.Y. Muhammad, M.K. Asad, K. Abdur Rahman, Z.Q. Irfan, K. Heinz-Bernhard, Zia-ur-R, Synthesis, spectroscopic characterization, DFT optimization and biological activities of Schiff bases and their metal(II) complexes, J. Mol. Struct. 1145 (2017) 132–140.

[15] Z.H. Chohan, M. Praveen, A. Ghaffer, Synthesis, characterisation and biological role of anions (nitrate, sulphate, oxalate and acetate) in Co(II), Cu(II) and Ni(II) metal chelates of some Schiff- base derived amino acids, Synth. React. Inorg. Met. 28 (1998) 1673–1687.

[16] G.Y. Nagesh, B.H.M. Mruthyunjayaswamy, Synthesis, characterization and biological relevance of some metal(II) complexes with oxygen, nitrogen and oxygen (ONO) donor Schiff base ligand derived from thiazole and 2-hydroxy-1-naphthaldehyde, J. Mol. Struct. 1085 (2015) 198–206.

[17] H.S. Çalık, E. Ispir, S. Karabuga, M. Aslantas, Ruthenium (II) complexes of NO ligands: synthesis, characterization and

application in transfer hydrogenation of carbonyl compounds, J. Organomet. Chem. 801 (2016) 122–129.
[18] N. Turan, K. Buldurun, Synthesis, characterization and antioxidant activity of Schiff base and its metal complexes with Fe(II), Mn(II), Zn(II), and Ru(II) ions: catalytic activity of ruthenium(II) complex, Eur. J. Chem. 9 (2018) 22–29.
[19] M. Sebastian, V. Arun, P.P. Robinson, A.A. Varghese, R. Abraham, E. Suresh, K.K.M. Yusuf, Synthesis, structural characterization and catalytic activity study of Mn(II), Fe(III), Ni(II), Cu(II) and Zn(II) complexes of quinoxaline-2-carboxalidine-2- amino-5-methylphenol, Polyhedron 29 (2010) 3014–3020.
[20] H. Dugas, C. Penney, Bioorganic Chemistry, Springer, New York, 1981, pp. 435–448.
[21] J.D. Margerum, L.J. Miller, Photochromism, Interscience, Wiley, New York, 1971, pp. 569–570.
[22] W.J. Sawodny, M. Riederer, Addition compounds with polymeric chromium(II)–Schiff base complexes, Angew. Chem. Int. Ed. Engl. 16 (1977) 859–860.
[23] R. Manikandan, P. Viswanathamurthi, M. Muthukumar, Ruthenium(II) hydrazone Schiff base complexes: synthesis, spectral study and catalytic applications, Spectrochim. Acta A Mol. Biomol. Spectrosc. 83 (2011) 297–303.
[24] H. Mitsuda, K. Yuasumoto, K. Iwami, Antioxidation action of indole compounds during the autoxidation of linoleic acid, Eiyo to Shokuryo 19 (1996) 210–214.
[25] I. Gülçin, Antioxidant and antiradical activities of L-carnitine, Life Sci. 78 (2006) 803–811.
[26] H.P. Wichi, Enhanced tumor development by butylatedhydroxyanisole (BHA) form the prospective of effect on forestomach and oesophageal squamous epithelium, Food Chem. Toxicol. 26 (1988) 717–723.
[27] M. Oyaizu, Studies on product of browning reaction prepared from glucoseamine, Jpn. J. Nut. 44 (1986) 307–315.
[28] I. Gülçin, S. Beydemir, I.G. Sat, Ö.İ. Küfrevioğlu, Evaluation of antioxidant activity of corneliancherry (Cornus mas L.), Acta Aliment Hung. 34 (2005) 193–202.
[29] M.S. Blois, Antioxidant determinations by the use of a stable free radical, Nature 26 (1958) 1199–1200.
[30] J.M. Gichumbi, H.B. Friedrich, B. Omondi, Structural and kinetic studies of the polymerization reactions of ε-caprolactone catalyzed by (pyrazol-1-ylmethyl) pyridine Cu (II) and Zn (II) complexes, J. Mol. Catal. A: Chem. 416 (2016) 29–38.
[31] M. Kalita, P. Gogoi, P. Barman, A new series of Ni (II), Cu (II), Co (II) and Pd (II) complexes with an ONS donor Schiff base: synthesis, crystal structure, catalytic properties and bioactivities, Polyhedron 74 (2014) 93–98.
[32] N. Raman, A. Kulandaisamy, K. Jeyasubramanian, Synthesis,, spectroscopic characterization, redox and biological screening of some Schiff base transition metal (II) complexes derived from salicylidene-4-aminoantipyrine and. 2-aminophenol/2-aminothiophenol, Synth. React. Inorg. Met. Org. Chem. 31 (2001) 1249.
[33] B. Anupama, M. Sunita, D. ShivaLeela, B. Ushaiah, C. GyanaKumari, Synthesis, spectral characterization, DNA binding studies and antimicrobial activity of Co (II), Ni (II), Zn (II), Fe(III) and VO(IV) complexes with 4-aminoantipyrine Schiff base of ortho-vanillin, J. Fluoresc. 24 (2014) 1067–1076.
[34] A.M.A. Alaghaz, Y.A. Ammar, H.A. Bayoumi, S.A. Aldhlmani, Synthesis,, spectral characterization, thermal analysis, molecular modeling and antimicrobial activity of new potentially. N_2O_2 azo-dye Schiff base complexes, Molecu. Struct. 1074 (2014) 359–375.
[35] R. Manikandan, P. Viswanathamurthi, M. Muthukumar, Ruthenium(II) hydrazone Schiff base complexes: synthesis, spectral study and catalytic applications, Spectrochim. Acta. A Mol Biomol. Spectrosc. 28 (2011) 297–330.
[36] M. Mishra, K. Tiwari, S.A. Kumar, V.P. Singh, Synthesis, structural and corrosion inhibition studies on Mn(II), Cu(II) and Zn(II) complexes with a Schiff base derived from 2-hydroxypropiophenone, Polyhedron 77 (2014) 57–65.
[37] B. Shafaatian, A. Soleymanpour, N.K. Oskouei, B. Notash, S. A. Rezvani, Synthesis, crystal structure, fluorescence and electro- chemical studies of a new tridentate Schiff base ligand and its nickel(II) and palladium(II) complexes, Spectrochim. Acta A Mol. Biomol. Spectrosc. 128 (2014) 363–369.
[38] R. Gup, B. Kırkan, Synthesis and spectroscopic studies of copper(II) and nickel(II) complexes containing hydrazonic ligands and heterocyclic coligand, Spectrochim. Acta A Mol. Biomol. Spectrosc. 62 (2005) 1188–1189.
[39] M. Shakir, Y. Azim, H.T.N. Chishti, S. Parveen, Synthesis, characterization of complexes of Co(II), Ni(II), Cu(II) and Zn(II) with 12-membered Schiff base tetraazamacrocyclic ligand and the study of their antimicrobial and reducing power, Spectrochim. Acta A Mol. Biomol. Spectrosc. 65 (2006) 490–496.
[40] M.M. Al-Mogren, M.A. Alaghaz Abdel-Nasser, E.A. Ebrahem, Synthesis,, spectroscopic, molecular orbital calculation, cytotoxic, molecular docking of DNA binding and DNA cleavage studies of transition metal complexes with N-benzylidene-NO-salicylidene-1, 1-diaminopropane, Spectrochim. Acta A Mol. Biomol. Spectrosc. 114 (2013) 695–707.
[41] G.G. Mohamed, M.A. Zayed, S.M. Abdallah, Metal complexes of a novel Schiff base derived from sulphametrole and varelaldehyde. Synthesis, spectral, thermal characterization and biological activity, J. Mol. Struct. 979 (2010) 62–71.
[42] K.P. Balasubramanian, R. Karvembu, R. Prabhakaran, V. Chinnusamy, K. Natarajan, Synthesis, spectral, catalytic and antimicrobial studies of PPh3/AsPh3 complexes of Ru(III) with dibasic tridentate O, N, S donor ligands, Spectrochim. Acta A Mol. Biomol. Spectrosc. 68 (2007) 50–54.
[43] P. Bharati, A. Bharti, M.K. Bharty, N.K. Singh, S. Kashyap, P. Singh Udai, R.J. Butcher, Cu(II), Zn(II) and Mn(II) complexes of NNS tridentate and Pd(II) complex of NN(μ-S) tetradentatethiobenzyl esters: synthesis, spectral and X-ray characterization, Polyhedron 97 (2015) 215–226.
[44] E. Tas, A. Kilic, M. Durgun, L. Küpecik, I. Yilmaz, S. Arslan, Cu (II), Co(II), Ni(II), Mn(II), and Fe(II) metal complexes containing N, N -(3,4-diaminobenzophenon)-3,5-B^{u}t 2-salicylaldimine ligand: synthesis, structural characterization, thermal properties, electrochemistry, and spectroelectrochemistry, Spectrochim. Acta A Mol. Biomol. Spectrosc. 2 (2010) 811–818.
[45] S. Dayan, N. Kayacı, N.O. Kalaycioglu, O. Dayan, E.Ç. Öztürk, Synthesis of ruthenium(II) complexes derived from reduced imine ligands: as catalysts for transfer hydrogenation of ketones, Inorg. Chim. Acta 401 (1) (2013) 07–113.
[46] K. Mounika, A. Pragathi, C. Gyanakumari, Synthesis¸ characterization and biological activity of a Schiff base derived from 3-ethoxy salicylaldehyde and 2-amino benzoic acid and its transition metal complexes, J. Sci. Res. 2 (2010) 513–524.
[47] S. Biswas, S. Jana, T.K. Monda, Osmium-hydride-carbonyl complex with thioether containing Schiff base ligand: synthesis, crystal structure, electrochemistry and catalytic transfer hydrogenation, J Organomet. Chem. 846 (2017) 201–207.
[48] V.R. Landaeta, A.D.S. La Rosa, R.E.R. Lugo, Transfer hydrogenation of ketones catalyzed by iridium-bulky phosphine complexes, Inorg. Chim. Acta 470 (2018) 303–311.
[49] A. Kilic, İ.H. Kaya, I. Ozaslan, M. Aydemirb, F. Durap, Catechol-type ligand containing new modular design dioxaborinane compounds: use in the transfer hydrogenation of various ketones, Catal. Commun. 111 (2018) 42–46.
[50] N. Kayaci, S. Dayan, N. Özpozan, Novel N-coordinate half-sandwich ruthenium(II) arene complexes bearing sulfonamide fragments: catalytic activities in the TH of acetophenone derivatives, J. Mol. Struct. 1099 (2015) 446–452.